Journal of Materials Science and Engineering A 8 (9-10) (2018) 209-221
doi: 10.17265/2161-6213/2018.9-10.006

Effects of pH on Au-Deposited TiO_2 for Catalytic Photoreduction of CO_2 with H_2O

Y. Y. Maruo, T. Kondoh and Y. Nakagawa

Faculty of Engineering, Tohoku Institute of Technology, Sendaishi, Miyagi 982-8577, Japan

Abstract: The photoreduction of CO_2 to hydrocarbons is a sustainable energy technology that not only reduces emissions but also the need for alternative fuels. In this study, Au nanoparticles were deposited on anatase TiO_2 using various pH controlled Au ion solutions (from pH = 6 to 9). Photoreduction experiments were performed in an FT-IR gas reactor using CO_2 gas with 50% relative humidity as the reactant for the four Au/TiO_2 samples. CH_4 was mainly detected as the CO_2 reduction product, along with a small amount of CO. The amounts of CH_4 produced normalised by Au weight were 437 ppm (pH 6), 664 ppm (pH 7), 1,040 ppm (pH 8) and 2,356 ppm (pH 9). Therefore, the pH of the solution used in Au nanoparticle deposition strongly influenced the amount of CH_4 produced. The highest production efficiency was obtained when the pH of the solution was 9. Considering the experimental results, we performed X-ray photoelectron spectroscopy and transmission electron microscope measurements and found that Au particle size was influenced by the pH of the solution with the size at pH 9 being smaller than that at pH 6. It was also found that there were Au-O states at the interface of Au nanoparticles and anatase TiO_2.

Key words: Au nanoparticle, Au/TiO_2, photoreduction, CO_2, methane.

1. Introduction

Atmospheric concentrations of greenhouse gases have increased dramatically. This increase is the primary cause of global warming and climate change. Release of carbon dioxide (CO_2) from fossil fuel combustion is the major contributor to this phenomenon; therefore reduction of CO_2 is an issue currently drawing the attention of many researchers. The reduction of CO_2 by photocatalysts is the preferred method to recycle CO_2 as a useful compound using energy input from cheap and abundant sources (e.g. solar energy) at room temperature and ambient pressure. This process utilizes ultraviolet (UV) and/or visible light as an excitation source for semiconductor catalysts. The photoexcited electrons can then reduce CO_2 with H_2O on the catalyst surface and form energy-bearing products such as CO, CH_4 and methanol. A variety of photocatalytic semiconductors have been studied; among them, TiO_2 is considered the most convenient candidate [1-7]. The advantages of TiO_2, such as low operation temperature, low cost and high stability, have led to relevant applications towards photocatalytic reduction of CO_2. However, TiO_2 exhibits a relatively high energy bandgap (3.2eV) and can only be excited by high energy UV irradiation, as well as relatively low CO_2 conversion efficiency. Increased CO_2 conversion efficiency was observed when the TiO_2 surface was loaded with metals, which function as "charge-carrier traps" and suppress recombination of photoexcited electron–hole pairs [8-15]. Ishitani et al. [16] reported that CO_2 photoreduction using Pd, Rh, Pt, Au, Cu and Ru deposited on TiO_2 by the photochemical deposition method produces CH_4 and CH_3COOH with Pd/TiO_2, Rh/TiO_2 and Cu/TiO_2. Li et al. [17] reported that the addition of Cu deposited on mesoporous silica was identified as Cu_2O and markedly increased the overall CO_2 conversion efficiency, as well as the selectivity to CH_4. Koci et al. [18] reported that CO_2 photoreduction using silver-doped TiO_2 mainly produced CH_4. Kubo

Corresponding author: Yasuko Yamada Maruo, professor, research fields: nano materials, analytical chemistry, chemical sensors.

et al. [19, 20] reported that Au nanoparticles acted like a dye and adsorbed visible light because it caused local surface plasmon absorption and specific properties for Cu, Ag and Au. Haruta et al. [21] prepared Au nanoparticles using several methods and made an Au/TiO_2 structure. They reported that Au nanoparticles deposited on easily reducible metal oxide, such as TiO_2, worked as a photo-oxidation catalyst, even though Au is generally stable and displays no catalytic performance [21]. Tatsuma et al. [22] reported that Au electrons in the Au/TiO_2 structure were excited by light in the IR-vis range, causing the electrons to move from Au to TiO_2, which is a great advantage for use of Au/TiO_2in solar batteries. In this study, we focused on the pH conditions of the solution used for Au nanoparticle deposition and considered the relationship between pH values and Au particle size. Furthermore, we performed photoreduction measurements of CO_2 to hydrocarbon and consider the relationship between the photoreduction catalytic efficiencies and pH of the solution.

2. Experimental

2.1 Catalyst Preparation

Anatase TiO_2 was purchased from Kanto-Kagaku (Japan) and used without further purification. The crystal structure of anatase TiO_2 was confirmed by X-ray diffraction (XRD) spectroscopy. Typical deposition process of Au nanoparticles on TiO_2 was performed as follows. Hydrogen tetrachloroaurate (III) tetrahydrate (0.04 g) was dissolved in water (58 mL) and NaOH solution (0.1 mol/dm^3) was added until the desired pH was reached. Four different solutions from pH 6 to pH 9 were prepared and used. The anatase TiO_2 particles were added to the pH controlled Au(III) ion solution and stirred for 1 h. The white, cloudy solution of TiO_2 particles became alight violet, cloudy solution, indicating that the violet coloured Au nanoparticles were deposited on the TiO_2 powder. The obtained light violet powder was filtered and dried under nitrogen without humidity for 24 h. The dried powder was then sintered at 400 °C for 2 h, affording a violet powder.

The Au/TiO_2 catalyst was loaded as a thin film on a glass fibre filter (2 cm × 2 cm) and used in the photocatalytic reaction. It was prepared as follows; a select amount of Au/TiO_2 powder was first dispersed in methanol and then evenly loaded on a glass fibre filter, followed by drying under nitrogen atmosphere for 24 h. TiO_2 catalyst without Au was also prepared by loading anatase TiO_2 powder on a glass fibre filter. The amount of catalyst deposited on the glass fibre filter was 25 ± 5 mg in all cases.

2.2 Catalyst Characterization

XRD patterns of the powders were recorded with a MiniFlexII diffractometer (RIGAKU, Japan) using Cu-Kα radiation (λ = 0.1542 nm) in the range of 20–70° (2θ) with a step size of 0.05°. X-ray fluorescence (XRF) spectroscopy was performed using an EA6000VX (SII, Japan) and the amounts of Ti and Au were calculated from the intensity of the Kα and Lα lines at 4.51 keV and 9.70 keV, respectively. A diffuse reflectance UV-vis spectrometer (U-4100, Hitachi) was used to obtain UV-vis spectra, with bandgap values estimated by Kubelka-Munk conversion of the spectra. X-ray photoelectron spectroscopy (XPS) was performed with a PHI XPS5700 system using Al-Kα radiation (1486.6 eV). The photoelectron spectra were measured for Au4f, O1s, Ti2p and C1s core levels. Surface images of the samples were obtained using a scanning electron microscope (SEM) (SU1510, Hitachi, Japan) and transmission electron microscope (TEM) (JEM-2100F, JEOL).

2.3 Photocatalytic Reaction

A gas-phase FT-IR reactor system was designed for photocatalytic reactions. The Au/TiO_2 coated on glass fibre filter was installed in the gas reactor. A high pressure Hg lamp (Ushio-denki Co., Japan) was the

irradiation source. The light intensity of the lamp at the catalyst location was measured by a light power metre and found to be 4,200 μw/cm^2 for 250 nm < λ < 380 nm. Since the Hg lamp was shielded by Pyrex glass, light under 300 nm was removed. Compressed CO_2 (99.99%, Suzuki-shokan, Co.) controlled by a mass flow controller was passed through a water bubbler to generate a mixture of CO_2 and water vapour. The reactant gas with 50% relative humidity was then introduced into the gas reactor with BaF_2 windows on both sides. The inner cavity was 10 cm in diameter 3 cm (volume: 75 mL).

The concentrations of produced gases (e.g. CO, CH_4, CH_3OH) from the photoreduction reaction were measured every hour using a FT-IR spectrometer (iS-10, Thermo). The experimental system was a batch system, not a flow system.

CO and CH_4 concentrations were calculated from the intensities at 2,165 cm^{-1} and 3,014 cm^{-1} vibration absorbance, respectively. The calibration curves between CO and CH_4 concentration and the intensities at 2,165 cm^{-1} and 3,014 cm^{-1} vibration absorbance were prepared in the range of 1–50 ppm. This was carried out using several concentrations of diluted gases; 100 ppm CO standard gas and 1 % CH_4 standard gas, both diluted with nitrogen gas, respectively.

3. Results and Discussion

3.1 Characterization of Catalysts

We measured the XRD patterns of the Au/TiO_2 catalysts produced from pH 6 to pH 9 solutions. All patterns clearly showed anatase phases of TiO_2 with no detection of Au diffraction patterns. These results indicate that the catalyst preparation process did not affect the phase of TiO_2 particles. Diffraction peaks of Au species were not detected, indicating Au was either in low concentration or extremely small Au clusters. Fig. 1 shows the SEM images of the four Au/TiO_2 catalysts and anatase TiO_2. It also shows that the deposition of Au did not affect the crystalline structure of TiO_2. We performed high resolution SEM image measurement and simultaneous SEM-electron probe microanalysis (SEM-EPMA) for Au/TiO_2 (pH 6)

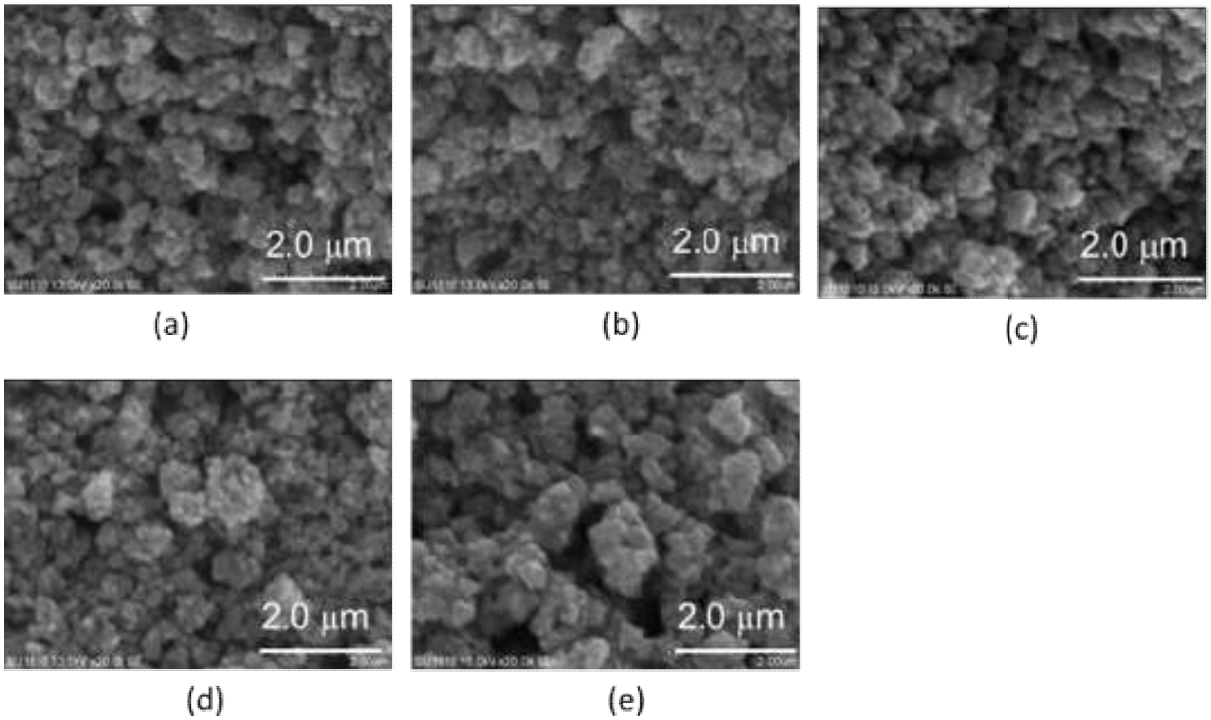

Fig. 1 SEM images of Au nanoparticles deposited on TiO_2 using several pH solutions; (a) pH 6, (b) pH 7, (c) pH 8, (d) pH 9, (e) anatase TiO_2.

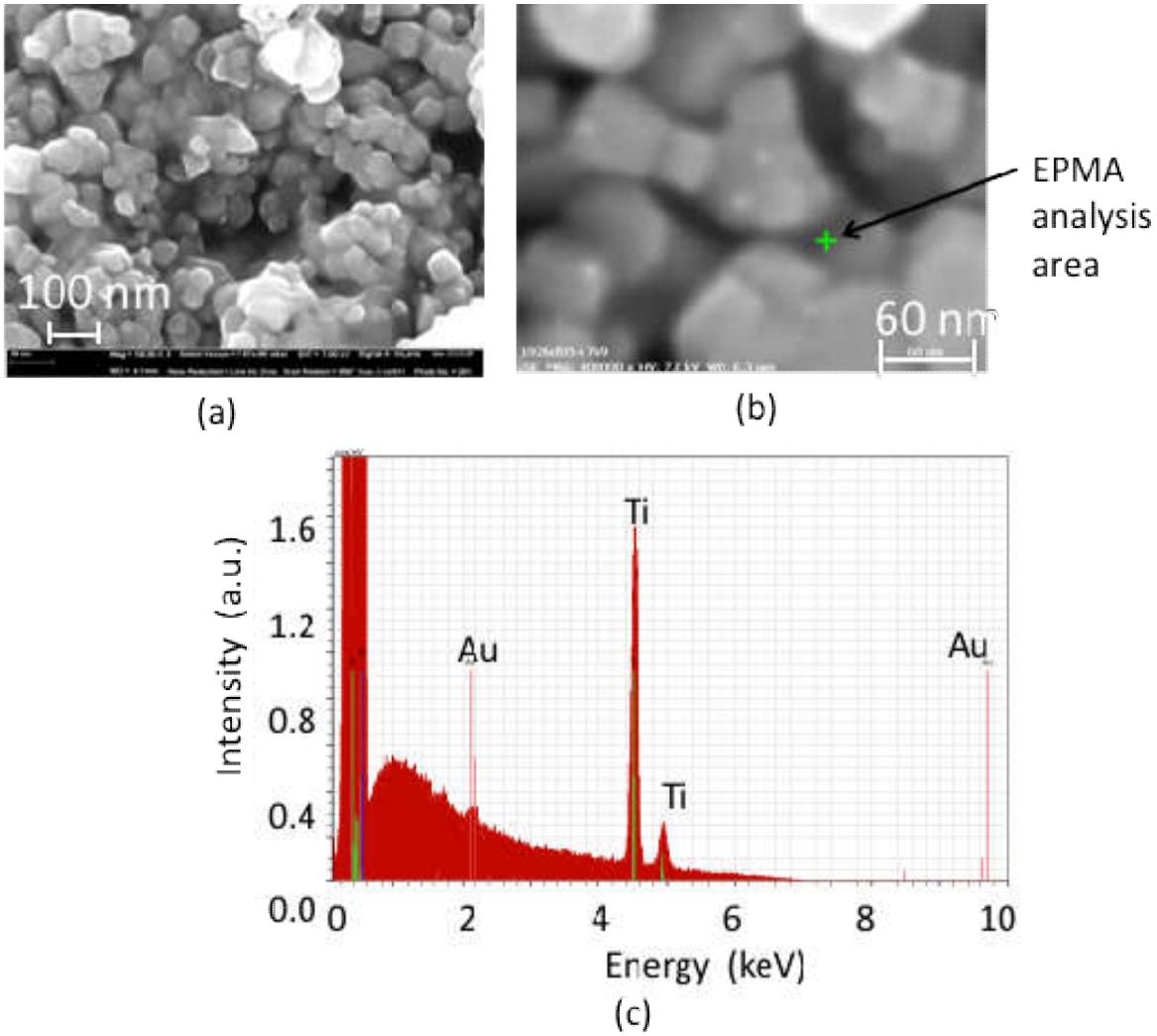

Fig. 2 High resolution SEM images of Au nanoparticles deposited on TiO_2 using the pH 6 solution and SEM-EPMA spectrum. (a) HR-SEM image of Au nanoparticles deposited on TiO_2 using the pH 6 solution, (b) HR-SEM image, "+" indicates the area for SEM-EPMA analysis, (c) SEM-EPMA spectrum. The positions of Ti and Au are indicted by lines.

catalyst, as shown in Fig. 2. No individual Au particles were observed in the images; however, Au signals around 2.2 keV were obtained from the EPMA results.

Table 1 lists the Au Lα and Ti Kα intensities obtained by XRF analysis. The Au Lα and Ti Kα were 9.71 keV and 4.51 keV, respectively. Since XRF is a surface-sensitive analysis method, we could successfully detect the Au signal. The intensity ratio of Au/Ti is also shown in Table 1. Elemental analysis using inductively coupled plasma atomic emission spectroscopy (ICP-AES) radiation was performed for the Au/TiO_2 (pH = 8) sample, and the obtained weight percentage values of Ti and Au were 59 and 0.6%, respectively. Therefore, the Au weight percentage of Au/TiO_2 (pH 6, pH 7, and pH 8) was approximately 0.6%. For Au/TiO_2 (pH 9), the intensity ratio of Au/Ti was 1/100 and the XRF intensity was proportional to the concentration; therefore an Au weight percentage of 0.14% was calculated from the XRF and elemental analysis results.

The diffuse diffraction UV-vis spectra of the catalysts are shown in Fig. 3. The catalysts absorb light below 400 nm, corresponding to a bandgap of approximately 3.0 eV. The 600 nm absorbance was caused by Au nanoparticles, because the violet color of

Table 1 Au Lα and Ti Kα intensities obtained from XRF analysis.

Element	Sample preparation pH			
	6	7	8	9
Au	13.6	16.2	14.4	3.3
Ti	282.3	348.1	335.1	342.6
Ti/Au	20.8	21.5	23.3	104

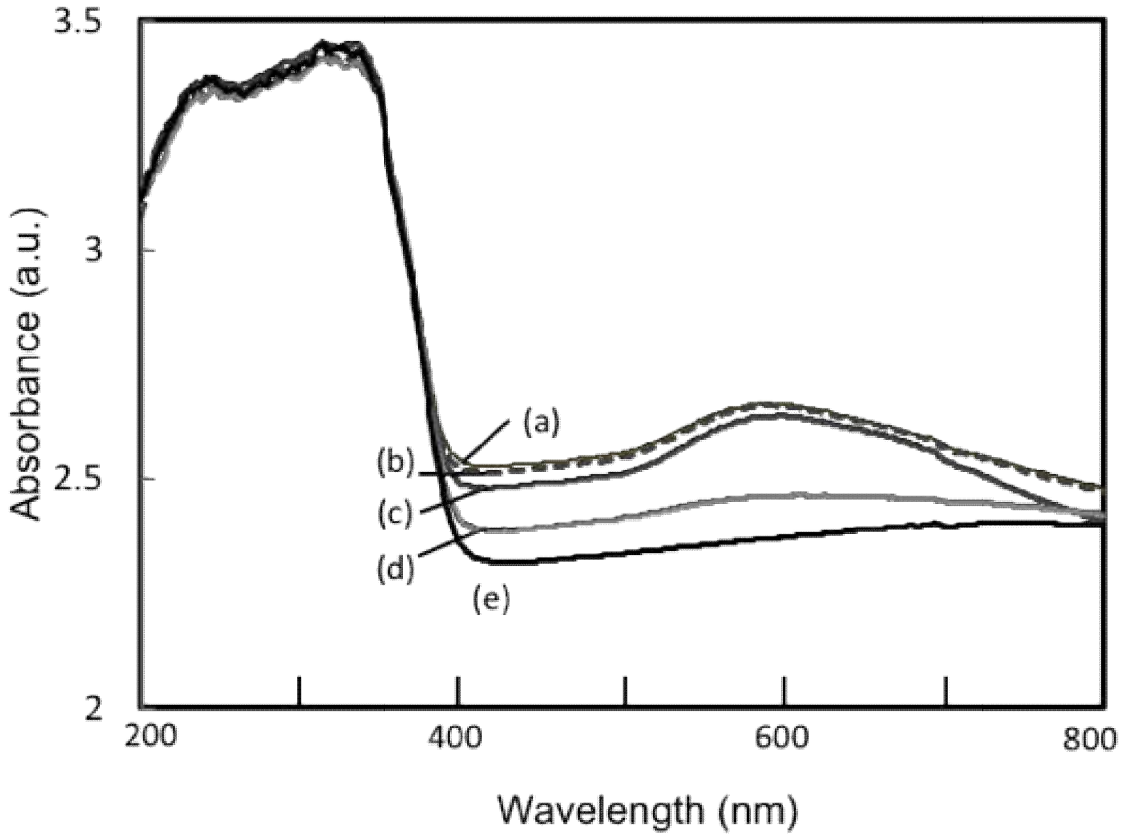

Fig. 3 Diffuse diffraction UV-vis spectra of Au nanoparticles deposited on TiO_2 using several pH solutions; (a) pH 6, (b) pH 7, (c) pH 8, (d) pH 9, (e) anatase TiO_2.

the Au nanoparticles caused surface Plasmon resonance [20]. There was no significant difference between the spectra of Au/TiO_2 (pH 6), Au/TiO_2 (pH 7), and Au/TiO_2 (pH 8), indicating nearly identical concentrations of Au. However, the lower absorbance at 600 nm for Au/TiO_2 (pH 9) indicated a lower concentration of Au than the other three Au/TiO_2 samples. These results corresponded with the XRF results.

The XPS spectra for Ti2p, O1s and Au4f of Au/TiO_2 (pH 6 and pH 9) are shown in Figs. 4-6, respectively. The O1s spectra of anatase TiO_2 and Au/TiO_2 (pH6) are also shown in Fig. 7 in order to compare the difference between the chemical states of oxygen with and without Au nanoparticles. The binding energy of the Ti2p3/2 main peak was calibrated at 458.8 eV to correct the shifts caused by charging.

For Au4f, two peaks corresponding to 4f5/2 and 4f7/2 with binding energies approximately 87 eV and 83 eV were detected. Viskovskiy et al. [23] reported the relationship between Au4f binding energy and Au nanoparticle size, revealing that Au4f binding energy in nanoparticles with diameters smaller than 5 nm shifted

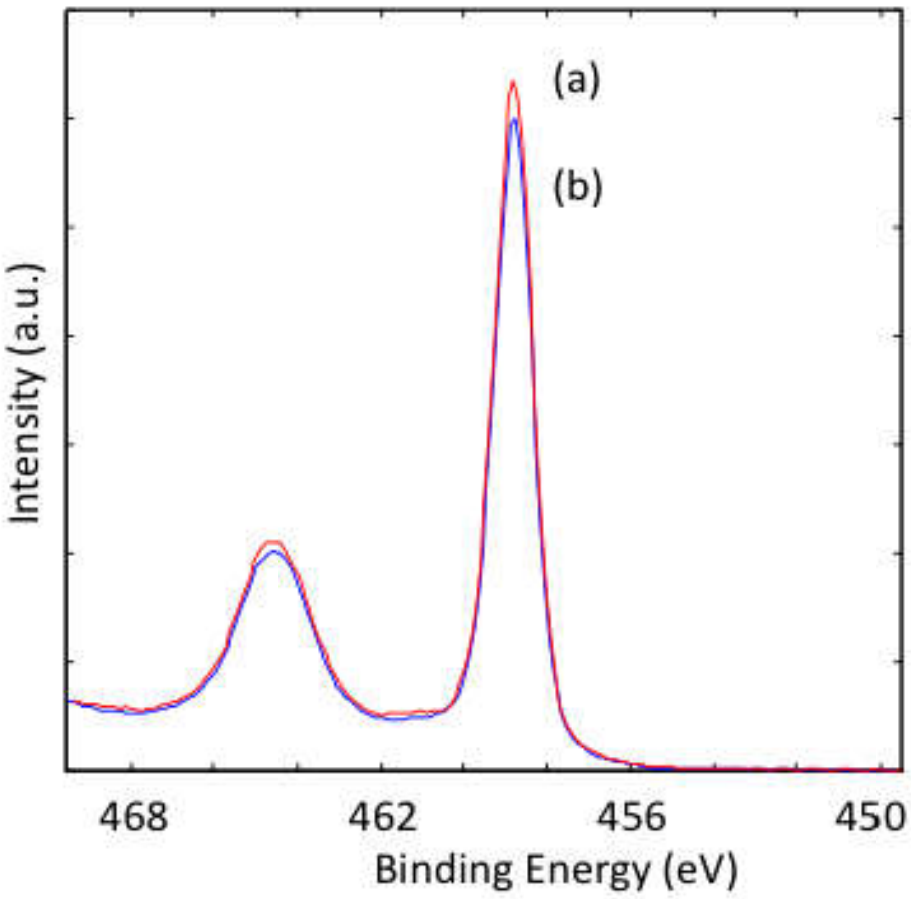

Fig. 4 Ti2p XPS spectra of Au nanoparticles deposited on TiO_2; (a) pH 6, (b) pH 9.

to higher binding energy of 0.4 eV. As shown in Fig. 6, we observed a binding energy shift of 0.3 eV for Au/TiO_2(pH 9). The synthesised Au particle size of the pH 6 sample would then be larger than that of the pH 9 sample.

For O1s spectra, there were three peaks in Au/TiO_2 (pH 6) with binding energies at 530.0 eV, 531.4 eV, and 532.5 eV as shown in Fig. 7. The two peaks with binding energies at 530.0 eV and 531.4 eV existed in anatase TiO_2, and the chemical states were estimated as Ti-O and O-H states, respectively. It was reported that the XPS chemical shift values had a linear relationship with the electron affinity values of neighboring atoms. The third peak in Au/TiO_2 (pH 6) at 532.5 eV is assumed to be the Au-O state, because the electron affinities of Ti, H, and Au are 1.5, 2.1 and 2.4, respectively. Therefore Au exists in the same vicinity as O at the interface between Au nanoparticles and TiO_2.

Since the Ti2p spectrum of Au/TiO_2(pH 6 and 9) is similar to that of anatase TiO_2, the Ti^{4+} single state exists, but not the Ti^{3+} state.

C1s spectra for both materials are shown in Fig. 8. The carbon source was atmospheric carbon compounds. The estimated relative amounts of carbon adsorbed on Au/TiO_2(pH 6) and anatase TiO_2 were 100 and 5, respectively. The amount adsorbed on Au/TiO_2 (pH 6) was twenty times greater than that of anatase TiO_2, indicating that the Au nanoparticle surface adsorbs volatile organic compounds.

We also carried out TEM measurement as shown in Fig. 9, and Au particles were observed from the TEM images. We selected five number of Au particles for each images, and measured average diameters of Au

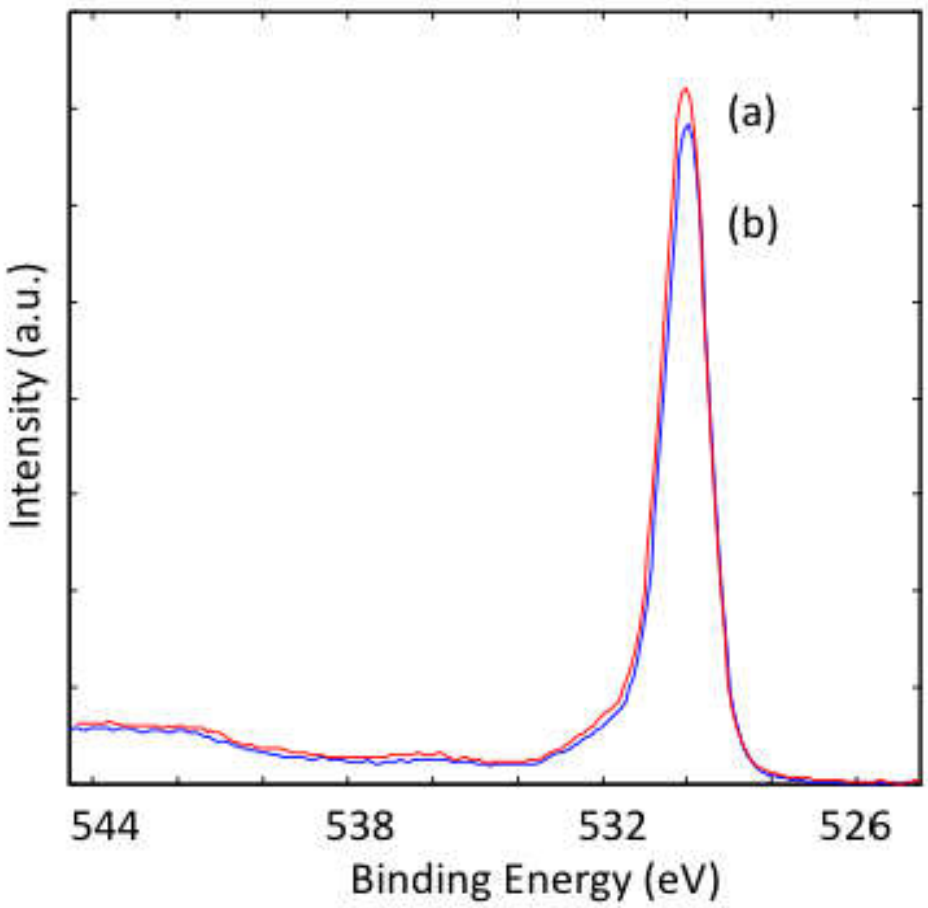

Fig. 5 O1s XPS spectra of Au nanoparticles deposited on TiO_2; (a) pH 6, (b) pH 9.

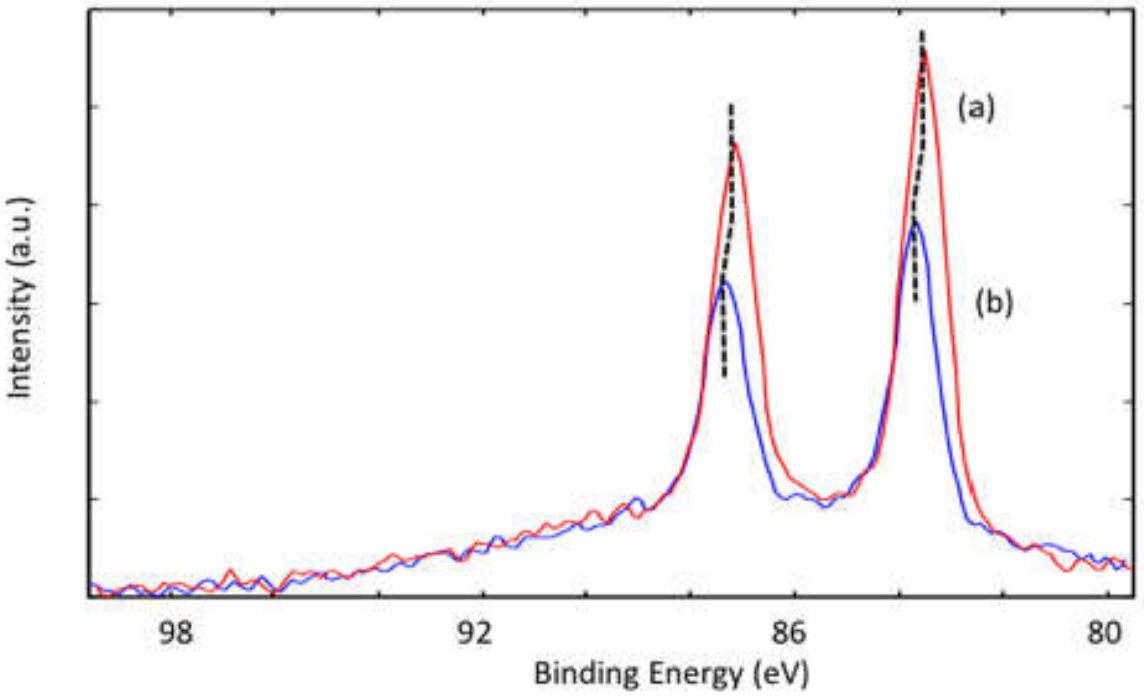

Fig. 6 Au4f XPS spectra of Au nanoparticles deposited on TiO_2; (a) pH 6, (b) pH 9.

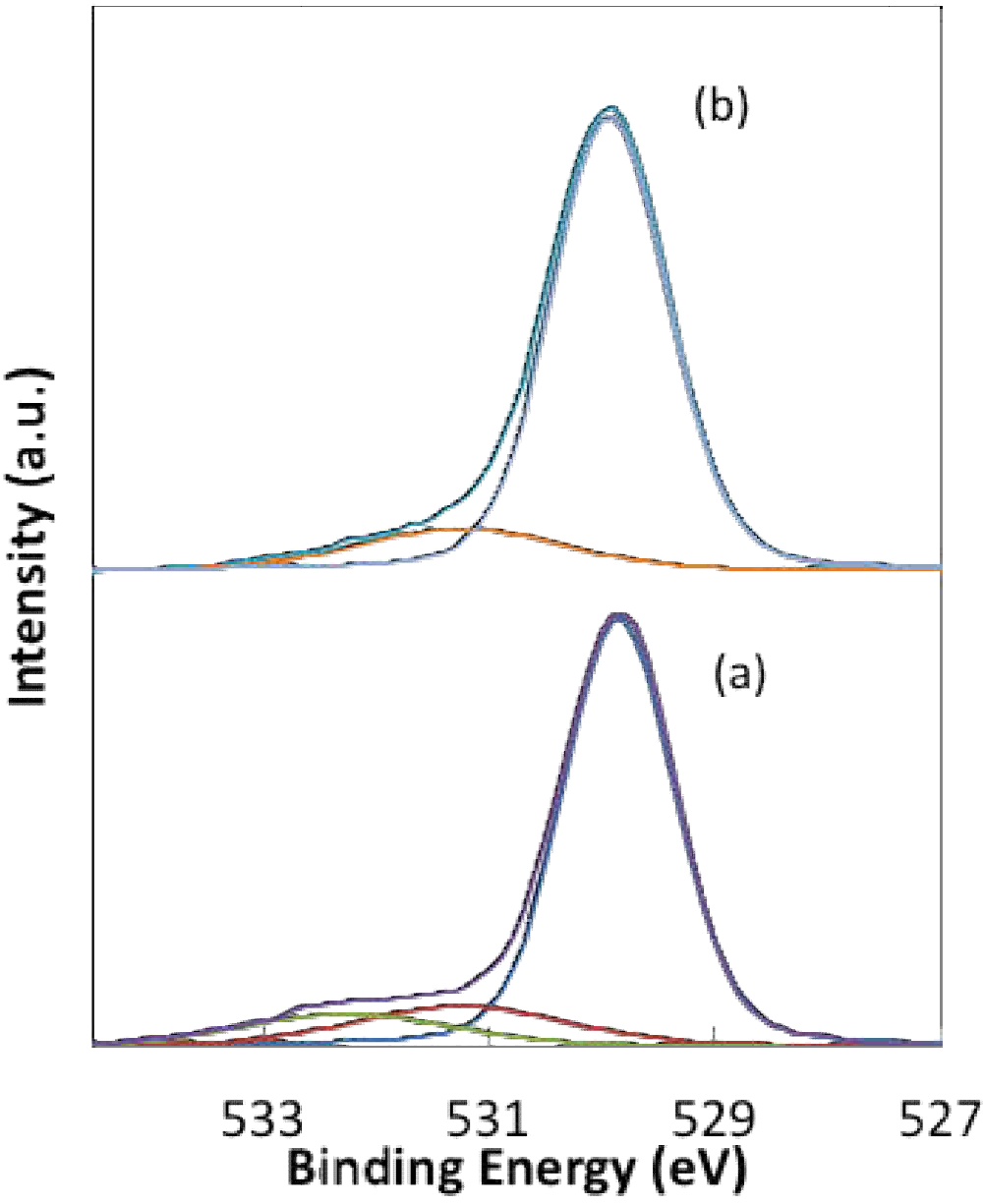

Fig. 7 Change in O1s XPS spectra of Au nanoparticles deposited on TiO_2 and anatase TiO_2; (a) Au nanoparticles deposited on TiO_2, (b) anatase TiO_2.

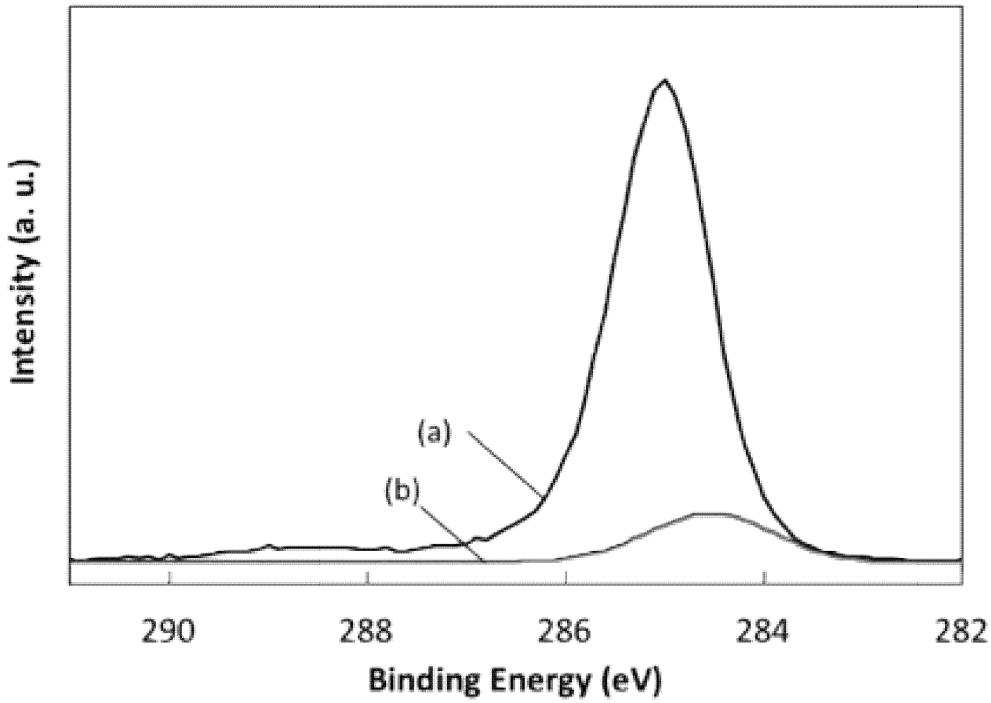

Fig. 8 Change in C1s XPS spectra of Au nanoparticles deposited on TiO_2 and anatase TiO_2; (a) Au nanoparticles deposited on TiO_2, (b) anatase TiO_2.

particles. Table 2 showed the measured diameters of Au particles, and it was found that Au particle size at pH 9 was smaller than that at pH 6.

3.2 Photocatalytic Reduction of CO_2

The effect of irradiation time on the formation of CO_2 photocatalytic reduction products was investigated over a period of 0–5 h. Two main products (CO and CH_4) were detected in the gas phases. Methanol, formic acid and formaldehyde were undetectable in the gas phase.

Comparison of CH_4 and CO yields over four different Au/TiO_2 samples are shown in Figs. 10 and 11, respectively. The yields of CH_4 and CO increased up to several hours after which someone gradually decreased. A similar trend of yield-time dependency was observed for all samples. It was reported that the Au/TiO_2 surface effectively adsorbs CO molecules [24]. Therefore, as we are not using a flow system, a gradual decrease in the amount of CH_4 would be caused by adsorption on the Au/TiO_2 surface.

Considering that CH_4 production using the anatase TiO_2 catalyst was low, the addition of Au nanoparticles will enhance CH_4 production. The CH_4 produced after 1 h of irradiation was normalised by Au amounts estimated by XRF analysis, with the calculated values shown in Table 3. The highest yield of CH_4 was obtained with Au/TiO_2 (pH 9), which increased when the pH was increased. The efficiency of CH_4 production with Au/TiO_2 was greatly dependent on the pH of the solution used during Au nanoparticle deposition. In this experiment, Au nanoparticles were deposited by solution method and it was assumed that the particle size was affected by the pH of the solution. Considering the XRF results, the Au layer of Au/TiO_2 (pH 9) was thinner than under other pH conditions and the colour of the sample was thinner violet than other samples. Therefore, it was assumed that the particle size of deposited Au on TiO_2 was affected by the pH of the solution, with smaller particle sizes being obtained under more alkaline conditions. The electronic structure of the Au and TiO_2 interface was reported by Tatsuma et al. [22]. Considering this state, the excited

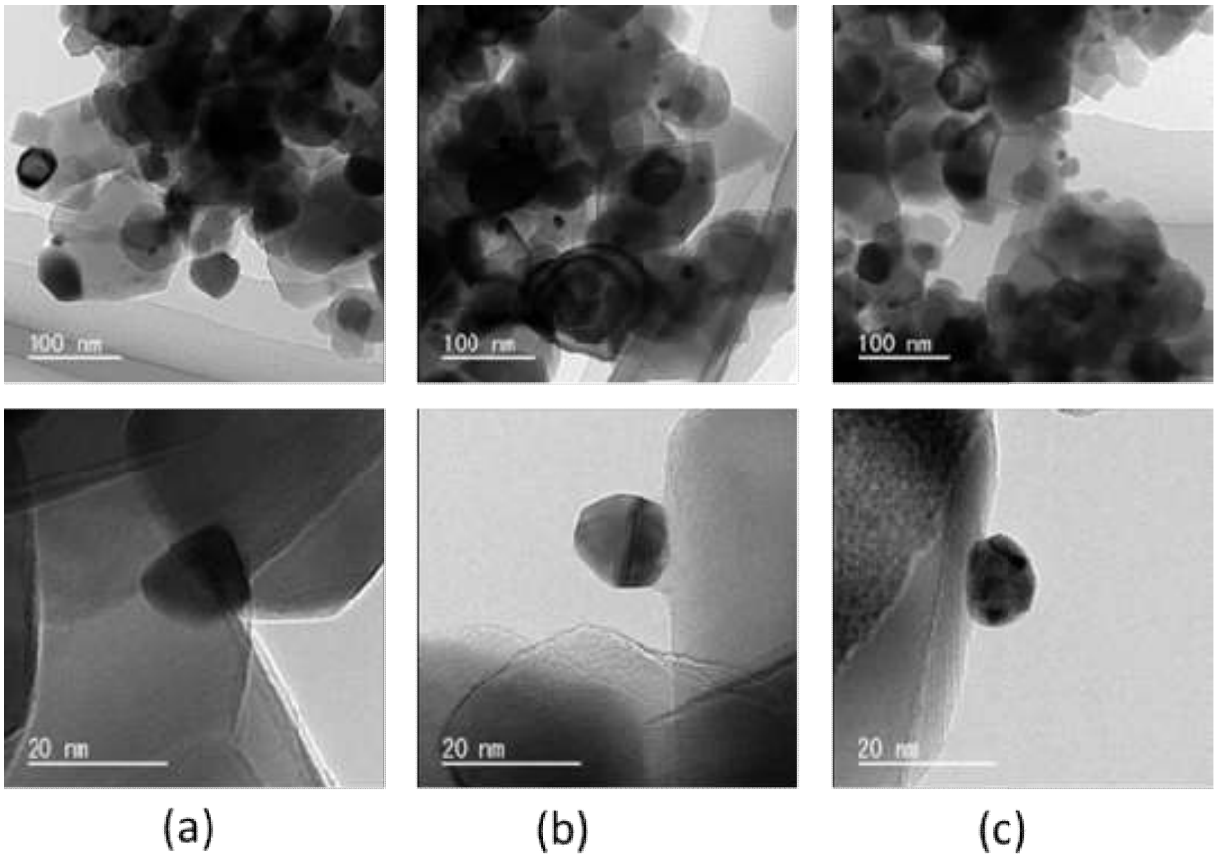

Fig. 9 TEM images of Au nanoparticles deposited on TiO_2 using several pH solutions; (a) pH 6, (b) pH 7, (c) pH 9.

Table 2 Particle size of deposited Au at several pH conditions.

pH	6	7	9
Size (nm)	15 ± 2	15 ± 2	10 ± 1

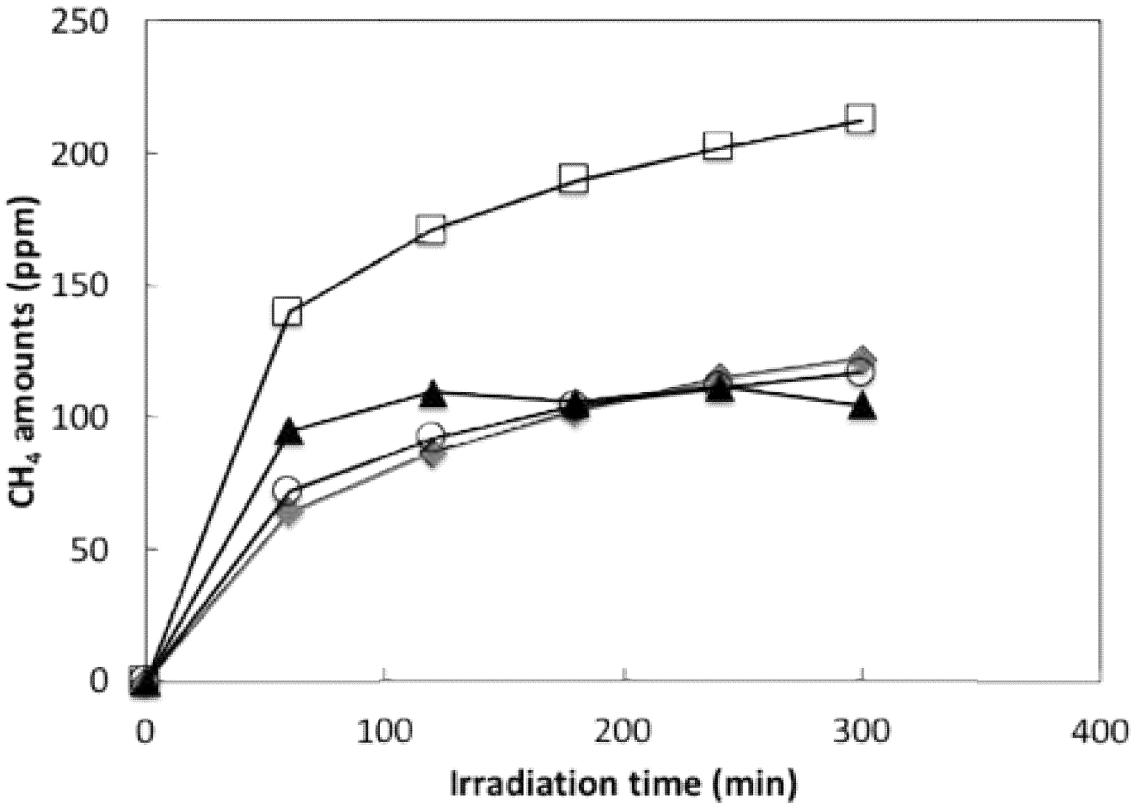

Fig. 10 Time dependence of CH_4 production for Au nanoparticles deposited on TiO_2 using several pH solutions; (a) pH 6, (b) pH 7, (c) pH 8, (d) pH 9.

photoelectrons will move from Au to TiO_2 and the resultant holes will move from TiO_2 to Au. Therefore, the electron-related reaction will occur on the TiO_2 surface and the hole related reaction will occur on the Au surface. The chemical reactions proposed for CH_4 and CO production from photoreduction of CO_2 with H_2O are as follows:

$$CO_2 + 8H^+ + 8e\text{-} \rightarrow CH_4 + 2H_2O$$

$$CO_2 + 2H^+ + 2e\text{-} \rightarrow CO + H_2O$$

For CH_4 production, eight electron–hole pairs have to react at the same time; therefore, the recombination time must be significantly longer than the electron–hole lifetime for CH_4 production to occur. The greater production rate of CH_4 with Au/TiO_2 (pH 9) indicates a longer lifetime than that of other pH samples. It was necessary that the electron transfer reaction occurs on the TiO_2 surface and the hole transfer reaction occurs on the Au surface simultaneously. Therefore, small particle size and small coverage of Au deposited on TiO_2 for Au/TiO_2 (pH 9) would work suited for both reactions.

Next, we focused on CO production. As shown in Fig. 11, CO was produced for up to several hours and someone followed by a gradual decrease. It was reported that CO was easily adsorbed on the Au/TiO_2 surface; therefore, the cause of the decrease would be the adsorption of CO on the Au/TiO_2 catalyst surface, as we did not use a flow system.

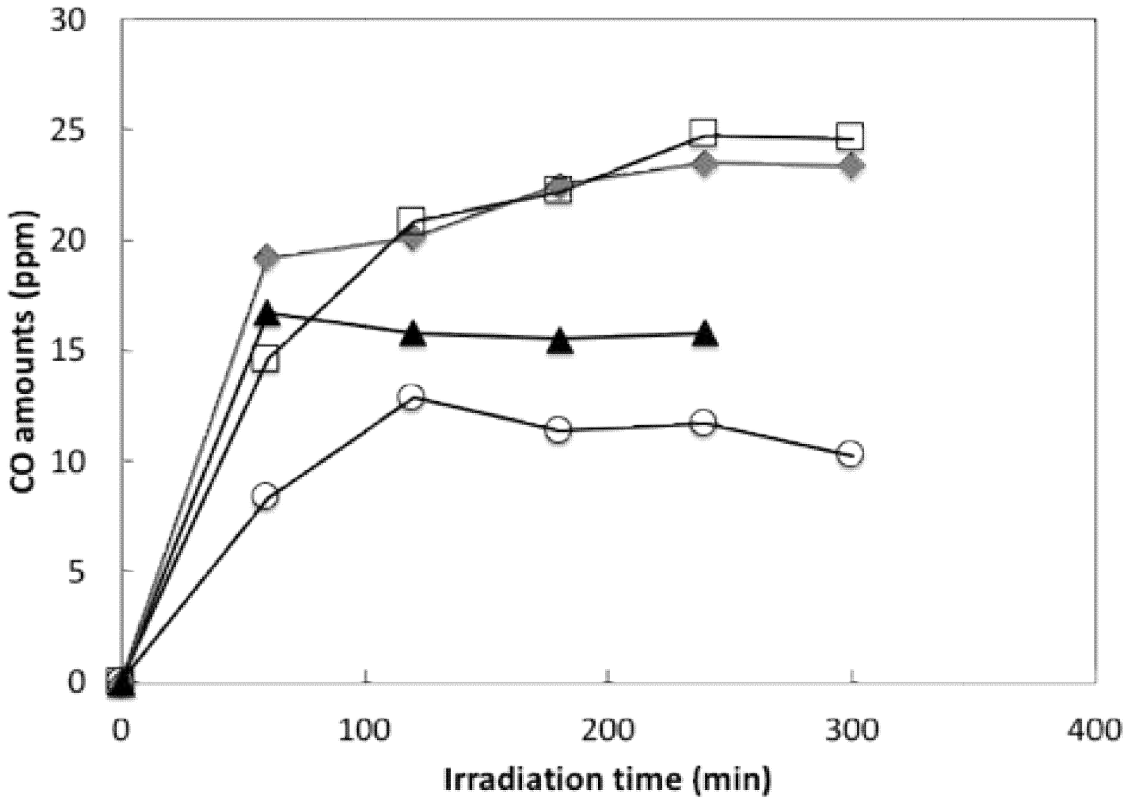

Fig. 11 Time dependence of CO production for Au nanoparticles deposited on TiO_2 using several pH solutions; (a) pH 6, (b) pH 7, (c) pH 8, (d) pH 9.

Table 3 Amounts of CH_4produced after 1 h irradiation normalised by Au weights estimated by XRF analysis.

	Sample preparation pH			
	6	7	8	9
CH_4 (ppm/Au-mg)	437	664	1,040	2,356

4. Conclusion

Several different samples of Au nanoparticles deposited on TiO_2 were synthesized using pH controlled solutions. We considered the photoreduction properties of Au/TiO_2 for CO_2 with 50% H_2O. The main product was CH_4 and the greatest efficiency was obtained when Au/TiO_2 was formed from pH 9 solution. Considering XPS and XRF analysis results, smaller Au nanoparticles were deposited under alkali conditions, which is well suited for CO_2 photoreduction to CH_4. Small particle size enhances the formation of CH_4 from CO_2 and H_2O, as this indicates a small distance between interface and surface. The electron and hole were transferred through the interface and the reaction occurred on the surface.

Acknowledgement

We would like to thank Dr. T. Yamada of NTT Energy and Environment Systems Laboratories for discussion about electron state in Au/TiO_2. We would also like to thank Dr. S. Kobayashi, Mr. K. Akaoka, and Mrs. K. Yanase for discussion about sample preparation methods.

References

[1] Kudo, A., and Miseki, Y. 2009. "Heterogeneous Photocatalyst Materials for Water Splitting." *Chem. Soc. Rev.* 38: 253-78.

[2] Sakthivel, S., Hidalgo, M. C., Bahnemann, D. W., Geissen, S.-U., Murugesan, V., and Vogelpohl, A. 2006. "A Fine Route to Tune the Photocatalytic Activity of

TiO_2." *Appl. Cata.* B 63: 31-40.

[3] Nishimura, A., Komatsu, N., Mitsui, G., Hirota, M., and Hu, E. 2009. "CO_2 Reforming into Fuel Using TiO_2 Photocatalyst and Gas Separation Membrane." *Catalysis Today* 148: 341-9.

[4] Koci, K., Obalova, L., Matejova, L., Placha, D., Lacny, Z., Jirkovsky, J., and Solcova, O. 2009. "Effect of TiO_2 Particle Size on the Photocatalytic Reduction of CO_2." *Appl. Cata. B* 89: 494-502.

[5] Xia, X.-H., Jia, Z.-J., Yu, Y., Liang, Y., Wang, Z., and Ma, L.-L. 2007. "Preparation of Multi-Walled Carbon Nanotube Supported TiO_2 and Its Photocatalytic Activity in the Reduction of CO_2 with H_2O." *Carbon* 45: 717-21.

[6] Koci, K., Matejka, V., Lacny, Z., Obalova, L., and Kovar, P. 2011. "Comparison of the Pure TiO_2 and Kaolinite/TiO_2 Composite as Catalyst for CO_2 Photocatalytic Reduction." *Catal. Today* 161: 105-9.

[7] Chen, L., Li, G., Gray, K. A., Graham, M. E., Gentner, D. R., and Dimitrijevic, N. M. 2009. "Photoreduction of CO_2 by TiO_2 Nanocomposites Synthesized through Reactive Direct Current Magnetron Sputter Deposition." *Thin Solid Films* 517: 5641-5.

[8] Tan, S. S., Zou, L., and Hu, E. 2006. "Photocatalytic Reduction of Carbon Dioxide into Gaseous Hydrocarbon Using TiO_2 Pellets." *Catalysis. Today* 115: 269-73.

[9] Nguyen, T. V., and Wu, J. C. S. 2008. "Photoreduction of CO_2 in an Optical-Fiber Photoreactor: Effects of Metals Addition and Catalyst Carrier." *Appl. Cata. A* 335: 112-20.

[10] Chen, S., Yu, X., Zhang, H., and Liu, W. 2010. "Preparation and Photocatalytic Activity Evaluation of Composite Photocatalyst Fe-TiO_2/TiO_2." *J. Electrochem. Soc*. 157: K96-102.

[11] Lianjun, L., Cunyu, Z., and Ying, L. 2012. "Spontaneous Dissociation of CO_2 to CO on Defective Surface of Cu(I)/TiO_{2-x} Nanoparticles at Room Temperature." *J. Phys. Chem. C* 116: 7904-47.

[12] Ning, W. W., Jin, A. W., Dariusz, N. M., Pratim, B., Balavinayagam, R., Somik, M., et al. 2012. "Size and Structure Matter: Enhanced CO_2 Photoreduction Efficiency by Size-Resolved Ultrafine Pt Nanoparticles on TiO_2 Single Crystals." *J. Am. Chem. Soc*. 134: 11276-81.

[13] Qianyi, Z., Ying, L., Tingting, G., and Jean, A. M. 2012. "Copper and Iodine Co-modified TiO_2 Nanoparticles for Improved Activity of CO_2 Photoreduction with Water Vapor." *Appl. Catal. B Environ*. 123-124: 257-64.

[14] Lianjun, L., Huilei, Z., Ying, L., and Fei, G. 2013. "Tailoring Cu Valence and Oxygen Vacancy in Cu/TiO_2 Catalysts for Enhanced CO_2 Photoreduction Efficiency." *Appl. Catal. B Environ*. 134-135: 349-58.

[15] Dan, K., Tie, T. J. Z., Fei, Y., Jieliang, Z., and Xiwen, Z. 2013. "Electrodeposited Ag Nanoparticles on TiO_2 Nanorods for Enhanced UV Visible Light Photoreduction CO_2 to CH_4." *Appl. Sur. Sci*. 277: 105-10.

[16] Ishitani, O., Inoue, C., Suzuki, Y., and Ibusuki, T. 1993. "Photocatalytic Reduction of Carbon Dioxide to Methane and Acetic Acid by an Aqueous Suspension of Metal-Deposited TiO_2." *J. Photochem. Photobiol. A* 72: 269-71.

[17] Li, Y., Wang, W. N., Zhan, Z., Woo, M. H., and Wu, C. Y. 2010. "Photocatalytic Reduction of CO_2 with H_2O on Mesoporous Silica Supported Cu/TiO_2 Catalysts." *P. Appl. Catal. B Environ.* 100: 386-92.

[18] Koci, K., Mateju, K., Obalova, L., Krejcikova, S., Lacny, Z., Placha, D., et al. 2010. "Effect of Silver Doping on the TiO_2 for Photocatalytic Reduction of CO_2." *Appl. Catal. B Environ.* 96: 239-44.

[19] Kubo, R. 1962. "Electronic Properties of Metallic Fine Particles." *J. Phys. Soc. Jpn.* 17: 975-86.

[20] Ghosh, S. K., and Pal, T. 2007. "Interparticle Coupling Effect on the Surface Plasmon Resonance of Gold Nanoparticles: From Theory to Applications." *Chem. Rev*. 107: 4797-862.

[21] Hutchings, G. J., and Haruta, M. 2005. "A Golden Age of Catalysis: A perspective." *Appl. Catal. A General* 291: 2-5.

[22] Tian, Y., Tatsuma, T., and Ame, J. 2005. "Mechanisms and Applications of Plasmon-Induced Charge Separation at TiO_2 Films Loaded with Gold Nanoparticles." *Chem. Soc.* 127: 7632-7.

[23] Viskovskiy, A., Matsumoto, H., Mitsuhara, K., Nakada, T., Akita, T., and Kido, Y. 2011. "Size Dependent Properties of Electronic d-Band of Gold Nano-clusters." *Phys. Rev. B* 83: 165428.

[24] Steyn, J., Pattrick, G., Scurrell, M. S., Hildebrand, D., and van der Lingen, E. 2008. "An Unconventional Au/TiO_2 PROX System for Complete Removal of CO from Non-reformate Hydrogen." *Gold Bulletin* 41: 318-25.